Experimental Study on Mixed-Mode (I–II) Fracture Toughness of Freshwater Ice

Yaozhong Xu[1,2] · Mao Zhou[1,2] · Xian Yi[3] · Wen Hua[1,2,4] · Jiuzhou Huang[1,2] · Wenyu Zhang[1,2] · Shiming Dong[1,2]

Abstract

In recent years, the issue of aircraft icing has gained widespread recognition. The breaking and detachment of dynamic ice can pose a threat to flight safety. However, the shedding and fracture mechanisms of dynamic ice are unclear and cannot meet the engineering needs of ice-shedding hazard assessment. Therefore, studying the fracture toughness of ice bodies has extremely important practical significance. To address this issue, this article uses a centrally cracked Brazilian disk (CCBD) specimen to measure the pure mode I toughness and pure mode II fracture toughness of freshwater ice at different loading rates. The mixed-mode (I–II) fracture characteristics of ice are discussed, and the experimental results are compared and analyzed with the theoretical values of the generalized maximum tangential stress (GMTS) criterion considering the influence of T-stress. The results indicated that as the loading rate increases, the pure mode I toughness and pure mode II fracture toughness of freshwater ice decrease, and the fracture toughness of freshwater ice is more sensitive to the loading rate. In terms of fracture criteria, the theoretical value of the ratio of pure mode II fracture toughness to pure mode I fracture toughness based on the GMTS criterion is in good agreement with the experimental value, while the theoretical value based on the maximum tangential stress (MTS) criterion deviates significantly from the experimental value, indicating that the GMTS criterion considering the influence of T-stress can better predict the experimental results.

Keywords Freshwater ice · Fracture criteria · Centrally cracked Brazilian disk (CCBD) · Mixed-mode (I–II) · Loading rate

1 Introduction

With the development of aircraft and aerospace technology, humans are increasingly venturing into deep space. During the flight of various types of aircraft, ice may dynamically accumulate on the wing surfaces of some aircraft, posing a significant safety hazard and threatening people's lives and property [1]. To study the shedding and fracture mechanisms of ice on wing surfaces, it is necessary to understand the fracture characteristics of ice. The fracture toughness of ice is a key indicator of its ability to resist crack initiation and propagation and is a vital mechanical property of ice.

In fracture mechanics, the stress intensity factor and T-stress are two important parameters that characterize the strength of the elastic stress field at the crack tip. Smith [2] introduced T-stress based on the maximum tangential stress (MTS) and first proposed the generalized maximum tangential stress (GMTS) criterion. In addition to the stress intensity factors K_I and K_{II}, the criterion also considers the influence of T-stress. Ayatollahi and Aliha et al. [3, 4] found that T-stress has a great influence on the crack propagation path and mixed-mode fracture toughness of brittle materials, and the GMTS criterion can significantly improve the prediction of the experimental results. Hua [5] also obtained the GMTS criterion considering T-stress through experimental research on the composite fracture toughness of rusty rock, which can effectively predict the experimental results. This

✉ Shiming Dong
  smdong@scu.edu.cn

1 Key Laboratory of Deep Underground Science and Engineering, Ministry of Education, College of Architecture and Environment, Sichuan University, Chengdu 610065, China

2 Failure Mechanics and Engineering Disaster Prevention Key Laboratory of Sichuan Province, Sichuan University, Chengdu 610065, China

3 China Aerodynamics Research and Development Center/Low Speed Aerodynamics Research Institute, Mianyang 621000, China

4 College of Mechanical and Electrical Engineering, Xichang University, Xichang 615000, China

demonstrates that the introduction of T-stress into the fracture criterion can improve the prediction of experimental results.

Some scholars have studied the fracture toughness of ice. Deng et al. [6] used Yellow River ice as the research material and employed the Brazilian test method to conduct loading tests on the ice at different temperatures, strain rates, and sizes. They discovered that the fracture toughness of Yellow River ice is closely related to strain rates. Within the range of $(10^{-5}–10^{-1})$ s^{-1}, the fracture toughness decreases with the increase of strain rate, while temperature and size have little effect on the fracture toughness of Yellow River ice. Zhang et al. [7] developed an improved low-temperature split-Hopkinson pressure bar system for measuring the dynamic characteristics of ice splitting. They measured the quasi-static and dynamic fracture toughness of freshwater ice at different loading rates and temperatures using the notched semicircular bending method and studied the effects of loading rates and test temperatures on the mode I dynamic initial fracture toughness of freshwater ice. They found that the initial fracture toughness of freshwater ice under dynamic loading exceeds the initial fracture toughness under quasi-static loading. Christmann et al. [8] used the four-point bending technique to determine the critical fracture toughness of 91 Antarctic bubble ice samples with densities ranging from 840 to 870 kg/m^3. The average fracture toughness and standard deviation of Antarctic bubble ice were determined to be 95.35 kPa·m$^{0.5}$ and $\pm$ 16.69 kPa·m$^{0.5}$, respectively. Kamio et al. [9] found that their experimental data on the fracture toughness of sea ice conformed to the Weibull statistical distribution through the fracture toughness and strength characteristics of the ice in the Notoro Lagoon connected to the Sea of Okhotsk near Hokkaido. They proposed a model that predicts changes in the fracture toughness of sea ice. This model is a function of the statistical distribution of the ice crystal size, effective surface energy, and the elastic constant of ice. The model's predicted fracture toughness distribution was in good agreement with the experimental cumulative probability of the fracture toughness of sea ice. The relationship between the fracture probability of sea ice and the stress intensity factor was established through the calculation of the Weibull stress of sea ice. Zhang et al. [10] used the semicircle bending method to study the mixed-mode fracture toughness and pure mode II fracture toughness of granular freshwater ice. The study found that with the increase of grain size, the fracture toughness values of pure mode II and mixed-mode generally showed a slow downward trend, while the changes of cracks in the mixed-mode were complex, which ultimately showed an asymmetric distribution of displacement field. Gao et al. [11] also took Yellow River ice as the research object and used a three-point bending test to measure the fracture toughness of columnar ice

and granular ice under different strain rates and temperatures. The test results showed that the fracture toughness of Yellow River ice ranged mostly between 30 kPa·m$^{0.5}$ and 130 kPa·m$^{0.5}$.

According to the above-mentioned studies, most of the research on the fracture toughness of ice focused on pure mode I, with a lack of research on pure mode II and mixed-mode, and there is also no specific range of fracture toughness values for pure mode II and mixed-mode. However, the fracture of ice is mainly of the mixed-mode, and studying the pure mode II and mixed-mode fracture toughness of ice can better meet the needs of the actual working conditions. The Brazilian test is an experimental technique for studying pure mode I, pure mode II, and mixed-mode (I–II) fractures of brittle materials, and the relevant theories are relatively complete [12–20]. Using the Brazilian test method to measure the fracture toughness of ice has the advantage of conveniently achieving pure mode I, pure mode II, and mixed-mode loading methods by changing the loading angle. Therefore, this article uses the Brazilian test method to determine the pure mode I, pure mode II, and mixed-mode fracture toughness of ice using centrally cracked Brazilian disk (CCBD) specimens, analyzes the effects of loading rate and loading angle on the fracture toughness of ice, and uses the GMTS criterion to predict and analyze the test results.

This paper aims to verify and complete the fracture mechanics properties of certain types of ice based on previous research by scholars and provide potential solutions to the issue of aircraft wing ice falling off and breaking in the future.

2 Experimental Method

2.1 Stress Intensity Factor of a Centrally Cracked Brazilian Disk (CCBD) Subjected to a Pair of Concentrated Radial Loads

As shown in Fig. 1, a centrally cracked Brazilian disk (CCBD) is subjected to a pair of concentrated radial loads F, with a loading angle of β. The thickness of the disc is B, the diameter is $2R$, and the crack length is $2a$. Dong et al. [12] obtained the analytical expression for the stress intensity factor of the CCBD under mixed-mode loading conditions using the weight function method, which can be expressed as:

$$K_{\mathrm{I}} = \sigma\sqrt{\pi a}\left[f_{11} + 2\sum_{i=1}^{n} A_{1i} f_{1i} \alpha^{2(i-1)} \right] \tag{1}$$

$$K_{\mathrm{II}} = 2\sigma\sqrt{\pi a}\sum_{i=1}^{n} A_{2i} f_{2i} \alpha^{2(i-1)} \tag{2}$$
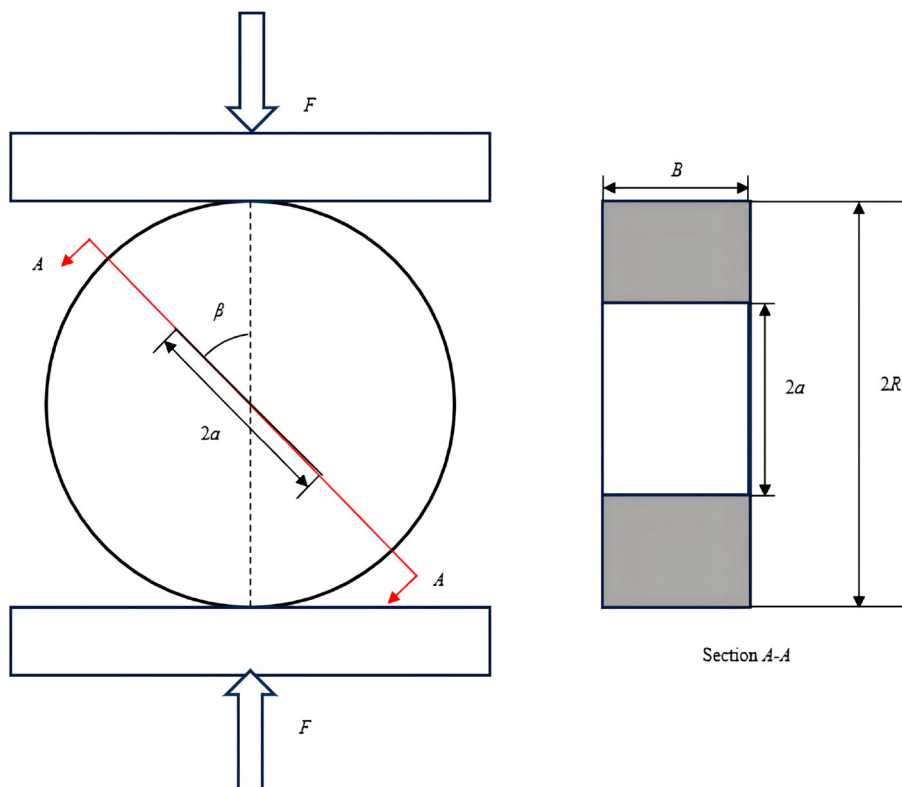
The dimensionless stress intensity factors F_I and F_{II} can be expressed as:

$$F_I = \frac{K_I}{\sigma\sqrt{\pi a}} = f_{11} + 2\sum_{i=1}^{n} A_{1i} f_{1i} \alpha^{2(i-1)} \tag{3}$$

$$F_{II} = \frac{K_{II}}{\sigma\sqrt{\pi a}} = 2\sum_{i=1}^{n} A_{2i} f_{2i} \alpha^{2(i-1)} \tag{4}$$

When the crack starts to propagate, $F = F_c$, where F_c is the critical load, and the pure mode I fracture toughness and pure mode II fracture toughness can be expressed as:

$$K_{IC} = \frac{F_c}{\pi B R}\sqrt{\pi a} f_{11}(\alpha) \tag{5}$$

$$K_{IIC} = \frac{2F_c}{\pi B R}\sqrt{\pi a}\sum_{i=1}^{n} A_{2i} f_{2i} \alpha^{2(i-1)} \tag{6}$$

In these equations, $\alpha = a/R$ is the relative crack length. The specific expressions for A_{2i}, A_{1i}, f_{2i}, and f_{1i} can be found in [12]. Following the suggestion for the value of term n in [12], with a prefabricated relative crack length of 0.5 in this experiment, when n is taken as 100, the accuracy of the calculation results already meets the requirements. Therefore, in all calculations in this article, the number of terms n is taken as 100.
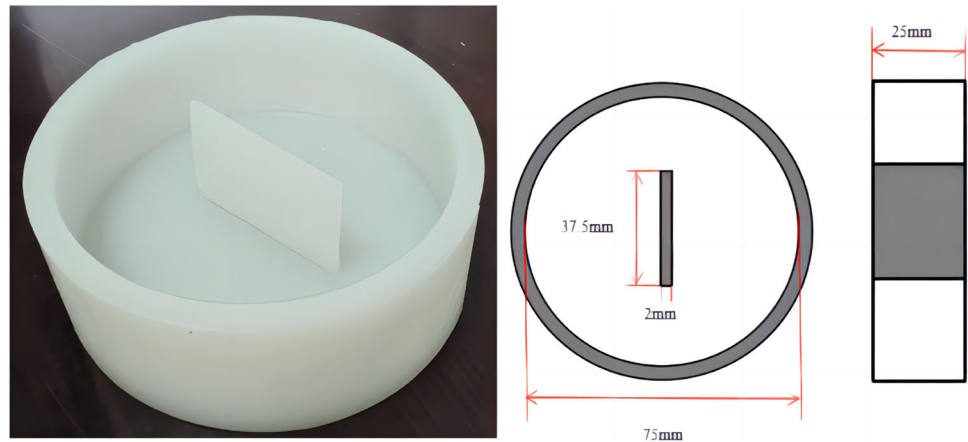
2.2 Preparation of Ice Specimens

The ice specimens used in this experiment were all prepared from freshwater ice. The ice mold is made of silicone material, preventing the ice from sticking to it. Consequently, the specimen can be easily extracted from the mold, guaranteeing the desired shape of the specimen. The mold has an inner diameter of 75 mm, a thickness of 25 mm, a crack length of 37.5 mm, a width of 2 mm, and a height of 25 mm, as shown in Fig. 2.

Figure 3 illustrates the preparation process. First, draw 80 ml of boiling water into a syringe and slowly inject it into the mold through a small hole in the lid. Next, place the specimen in the freezer, adjust the temperature to − 15 °C, and freeze it for 24 h. Afterward, remove the ice specimen from the mold, measure its geometric parameters, and place it in the freezer for testing.

As a brittle material, ice may contain microcracks, bubbles, and other defects in its internal structure, which significantly affect its mechanical properties [21]. To ensure the accuracy of experimental data, it is necessary to reduce the porosity inside the ice specimen. To reduce the porosity inside the prepared ice specimen, the boiling water injection method was used. First, an acrylic board was used as the cover of the mold, and two pinhole-sized holes were drilled on the cover using a manual electric drill. Water was then slowly injected from one small hole using a syringe, and the

Fig. 2 The ice mold for specimen preparation

Fig. 3 Specimen preparation process
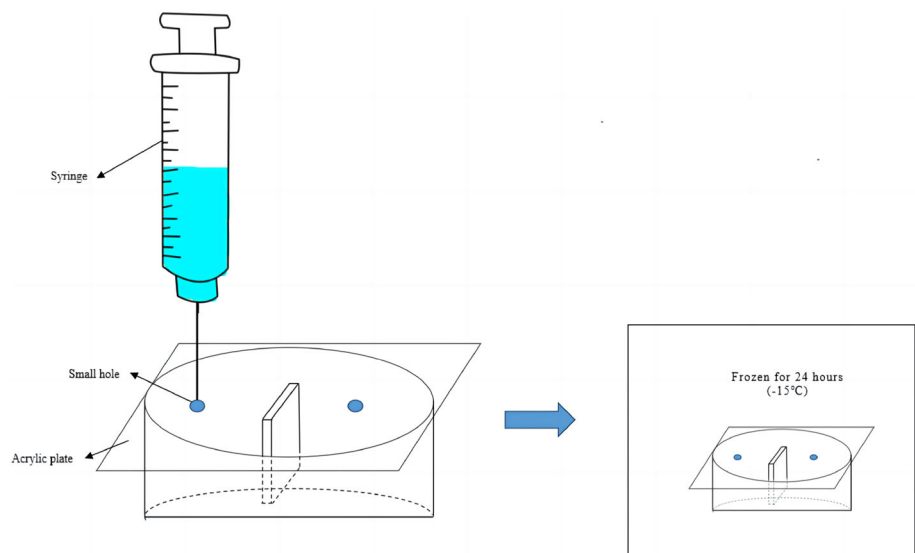
air inside the mold was discharged from the other small hole. This method can effectively reduce the air inside the mold, resulting in fewer bubbles and lower porosity in the produced ice specimen. The solubility of air in water decreases with increasing temperature, and using boiling water as a raw material can further reduce the porosity in an ice specimen.

This test was carried out in the Failure Mechanics and Engineering Disaster Prevention Key Laboratory of Sichuan Province, Sichuan University, using the electronic universal testing machine (DDL-300) produced by China Changchun Zhongji Test Equipment Co., Ltd. The loading method was displacement loading. This experiment fully considered the influence of environmental temperature and utilized low-temperature equipment to ensure a low-temperature environment. The experimental temperature and ice making temperature were both $-15\,°C$. CCBD specimens were used in the experiment, with a crack width of approximately 2 mm, a prefabricated diameter of 73.5 mm, a prefabricated thickness of 21.5 mm, and a prefabricated relative crack length of $\alpha = 0.5$. 80 specimens were designed and divided into 16 groups. Pure mode I loading rates were selected as 1, 1.5, 2, 2.5, 3, 10, 15, and 20 mm/min, while pure mode II loading rates were selected as 2, 2.5, 3, 4, 5, 10, 15, and 20 mm/min. The pure mode I fracture toughness and pure mode II fracture toughness of freshwater ice under different loading rates were measured. The average values of the geometric parameters of each specimen under pure mode I and pure mode II loading conditions are shown in Tables 1 and 2, respectively. The loading angle of the pure mode I crack generated by a CCBD specimen was $\beta = 0°$. When the relative crack length α is 0.5 or 0.51, the loading angle for generating pure mode II cracks is 22.93° [12]. Due to difficulties in angle control during actual testing, 23° was chosen as the loading angle. According to [22], the experimental error caused by an angle error of 0.1° to 0.5° is only 0.18% to 0.9%. Therefore, when selecting 23° as the critical loading angle for pure mode II crack fracture, the error can be ignored.

Table 1 Average values of geometric parameters of pure mode I specimens

| Loading rate v (mm/min)	Test piece thickness B (mm)	Specimen diameter $2R$ (mm)	Crack length $2a$ (mm)	Relative crack length α
1.0	21.75	73.53	37.09	0.504
1.5	21.42	73.66	37.43	0.508
2.0	21.53	73.39	37.32	0.509
2.5	21.28	73.66	36.96	0.502
3.0	21.87	73.29	37.01	0.505
10.0	22.28	74.06	36.94	0.499
15.0	22.46	74.16	37.02	0.499
20.0	22.68	74.08	36.94	0.499

Table 2 Average values of geometric parameters of pure mode II specimens

Loading rate v (mm/min)	Test piece thickness B (mm)	Specimen diameter $2R$ (mm)	Crack length $2a$ (mm)	Relative crack length α
2.0	21.58	73.69	36.96	0.502
2.5	21.64	73.58	37.15	0.505
3.0	21.47	73.72	37.16	0.504
4.0	21.68	73.76	37.10	0.503
5.0	21.52	73.80	37.18	0.504
10.0	22.74	74.18	37.06	0.500
15.0	22.60	74.18	37.08	0.500
20.0	22.62	74.08	37.06	0.500

3 Experimental Results

3.1 Experimental Results of Pure Mode I Fracture Toughness and Pure Mode II Fracture Toughness under Different Loading Rates

Figure 4 shows the load–displacement curves under different loading rates. The curves are initially concave due to the rupture of pores and bubbles inside the ice specimen under external forces. After compacting the ice specimen, the load and displacement approximate a linear relationship. Upon reaching its maximum value, the load rapidly decreases and unloads, which is in line with the typical fracture characteristics of brittle materials. Therefore, the maximum load of the specimen can be deemed as its critical failure load.

The maximum load obtained from the experiment was introduced into the pure mode I and pure mode II fracture toughness calculation formulas of the CCBD, and the pure mode I fracture toughness and pure mode II fracture toughness of freshwater ice at different loading rates were obtained. Tables 3 and 4, respectively, present the experimental results of pure mode I and pure mode II under different loading rates. According to Tables 3 and 4, the relationship between the pure mode I fracture toughness and pure mode II fracture
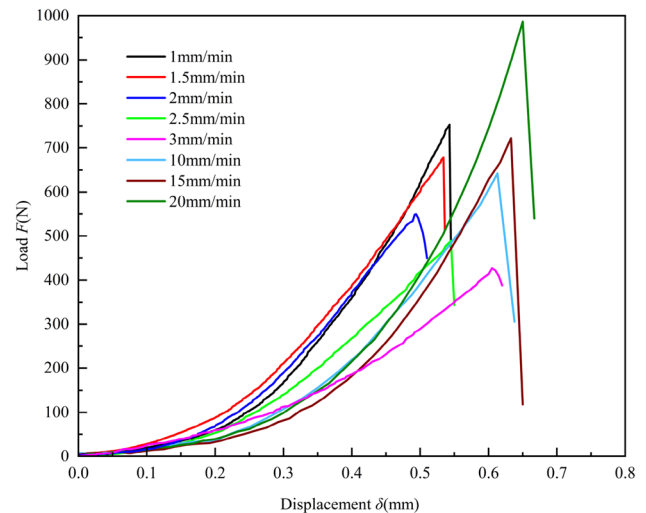
Fig. 4 Typical load–displacement curves

toughness of freshwater ice and the variation of loading rate can be obtained, as shown in Figs. 5 and 6, respectively. From Figs. 5 and 6, it can be seen that when the loading rates of freshwater ice are 1, 1.5, 2, 2.5, 3, 10, 15, and 20 mm/min, the average values of pure mode I fracture toughness K_{IC} are 137.80, 120.54, 113.18, 101.72, 91.34, 124.45, 137.28, and
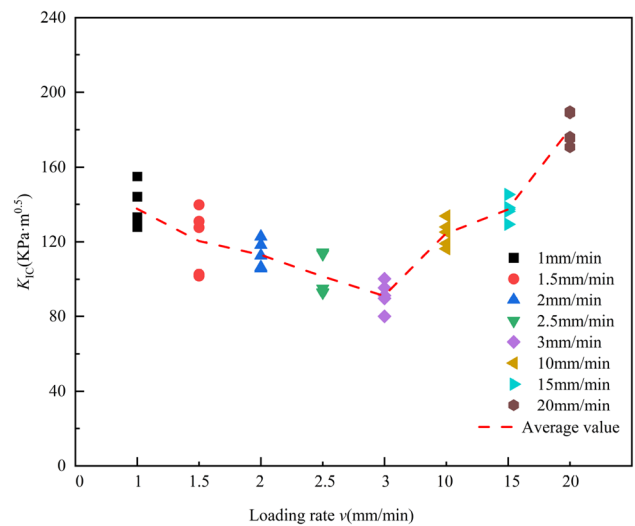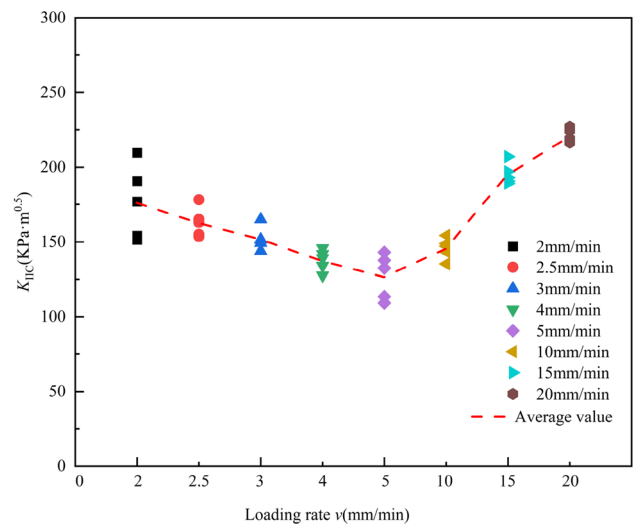
Table 3 Average values of pure mode I test results

Loading rate v (mm/min)	Maximum load F_c (N)	K_{IC} (kPa·m$^{0.5}$)
1	729.27	137.80
1.5	623.69	120.54
2	586.72	113.18
2.5	529.84	101.72
3	484.00	91.34
10	684.16	124.45
15	761.32	137.28
20	1012.18	180.14

Table 4 Average values of pure mode II test results

Loading rate v (mm/min)	Maximum load F_c (N)	K_{IIC} (kPa·m$^{0.5}$)
2	605.09	176.51
2.5	554.81	162.92
3	515.48	152.22
4	473.72	137.63
5	432.11	127.09
10	529.69	145.75
15	705.5	195.32
20	795.99	220.66

Fig. 5 K_{IC} at different loading rates

Fig. 6 K_{IIC} at different loading rates

180.14 kPa·m$^{0.5}$, respectively; when the loading rates are 2, 2.5, 3, 4, 5, 10, 15, and 20 mm/min, the average values of pure mode II fracture toughness K_{IIC} are 176.51, 162.92, 152.22, 137.63, 127.09, 145.75, 195.32, and 220.66 kPa·m$^{0.5}$, respectively. At the same loading rates of 2, 2.5, and 3 mm/min, the ratios of pure mode II fracture toughness to pure mode I fracture toughness, K_{IIC}/K_{IC}, are 1.56, 1.6, and 1.67, respectively. This can be seen from the load–displacement curves as well as the variations of fracture toughness at different loading rates, as shown in Figs. 4, 5, and 6. When the loading rate is 1 ~ 5 mm/min, as the loading rate increases, the peak load decreases, and the pure mode I fracture toughness and pure mode II fracture toughness both decrease. When the loading rate is 10 ~ 20 mm/min, with the increase of loading rate, the peak load increases, and the pure mode I fracture toughness and pure mode II fracture toughness both increase. The reason for this phenomenon is that the loading rate of 10 mm/min has exceeded the quasi-static range for the specimen size in this experiment. However, the dynamic fracture toughness of freshwater ice surpasses the quasi-static fracture toughness and increases with strain rate [7].

3.2 Experimental Results of Mode I Fracture Toughness and Mode II Fracture Toughness under Mixed-Mode Loading Conditions

The Brazilian test method allows for the convenient achievement of pure mode I, pure mode II, and mixed-mode loading conditions by changing the loading angle. In this experiment, a total of 6 groups of 18 specimens were set up, with a loading rate of 3 mm/min and loading angles of 0° (pure mode I), 5°, 10°, 15°, 20°, and 23° (pure mode II). The fracture toughness of freshwater ice under pure mode I, pure mode II, and mixed-mode loading conditions were measured. The geometric parameters of each specimen are shown in Table 5. The components of mode I fracture toughness and mode II fracture toughness of freshwater ice under different loading

Table 5 Geometric parameters of specimens under mixed-mode loading

Test piece number	Specimen diameter $2R$ (mm)	Crack length $2a$ (mm)	Test piece thickness B (mm)	The relative length of cracks α
M1	73.05	36.96	22.08	0.51
M2	72.46	36.72	21.85	0.51
M3	73.70	37.16	21.52	0.50
N1	73.90	37.10	21.60	0.50
N2	73.90	37.00	21.70	0.50
N3	73.90	37.00	21.60	0.50
P1	73.80	37.10	21.70	0.50
P2	73.80	37.10	21.70	0.50
P3	73.70	37.20	21.80	0.50
Q1	73.80	37.20	21.70	0.50
Q2	73.90	37.00	21.80	0.50
Q3	73.80	37.10	21.70	0.50
R1	73.90	37.00	21.70	0.50
R2	74.00	37.20	21.50	0.50
R3	74.00	36.80	21.50	0.50
S1	74.00	37.20	21.40	0.50
S2	73.37	37.16	21.43	0.51

Table 6 Test results under mixed-mode loading

| Test piece number	Loading angle β (°)	Maximum load Fc (N)	K_{I} (kPa·m$^{0.5}$)	K_{II} (kPa·m$^{0.5}$)
M1	0	477.72	90.03	0.00
M2	0	479.13	91.69	0.00
M3	0	500.00	94.93	0.00
N1	5	477.55	84.39	41.41
N2	5	500.22	87.87	43.12
N3	5	480.10	84.73	41.58
P1	10	552.12	78.99	90.59
P2	10	560.34	80.17	91.94
P3	10	473.91	67.67	77.61
Q1	15	580.71	54.73	131.80
Q2	15	576.21	53.84	129.65
Q3	15	480.18	45.19	108.84
R1	20	526.35	18.86	142.49
R2	20	562.95	20.38	154.02
R3	20	515.85	18.58	140.37
S1	23	516.12	0.00	151.62
S2	23	505.26	0.00	151.40
S3	23	504.30	0.00	149.24
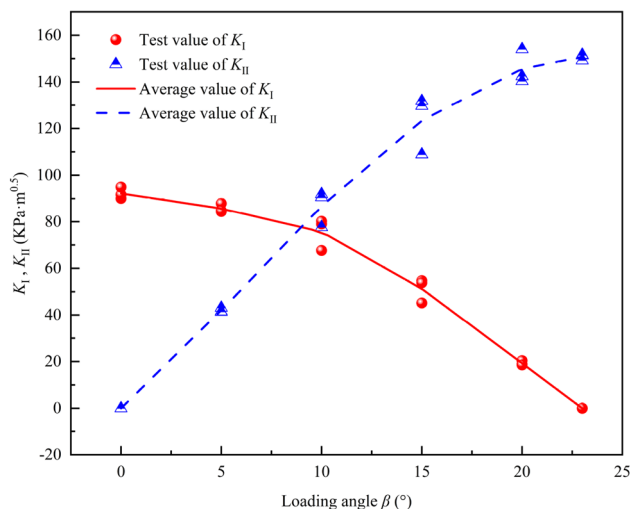
Fig. 7 Relationships between K_I, K_{II}, and loading angle β

angles can be calculated by substituting the maximum load obtained into the stress intensity factor formula of the CCBD under the mixed-mode loading condition. The test results are shown in Table 6. From Table 6, it can be seen that during mixed-mode loading, K_I and K_{II} vary with the loading angle β. Relationships between K_I, K_{II}, and loading angle variation are shown in Fig. 7. Under mixed-mode loading when the loading angles are 5°, 10°, 15°, and 20°, the average values of the mode I fracture toughness components of freshwater ice are 85.66, 75.61, 51.25, and 19.27 kPa·m$^{0.5}$, respectively; and the average values of the mode II fracture toughness components are 42.04, 86.71, 123.43, and 145.63 kPa·m$^{0.5}$, respectively. K_I decreases with the loading angle β, whileK_{II} increases with the loading angle β.

The fractured forms of specimens under mixed-mode loading conditions are shown in Fig. 8. When subjected to mixed-mode loading, the crack propagation path deviates from the direction of the prefabricated crack, forming a specific angle with it.

4 Predictive Analysis of Generalized Maximum Tangential Stress (GMTS) Criterion for Experimental Results under Mixed-Mode Loading Conditions

The mixed-mode fracture criteria mainly include the maximum tangential stress (MTS) criterion, the minimum strain energy density (SED) criterion, and the maximum energy release rate (MERR) criterion [23–29]. The MTS criterion is commonly used for mixed-mode fracture of brittle materials. However, some scholars have observed significant deviations between test values and theoretical values [2, 23–26]. Consequently, a generalized maximum tangential stress (GMTS)

criterion has been proposed based on the MTS criterion, taking into account the influence of T-stress [2, 23, 25, 30]. The elastic tangential stress component around the crack tip can be expressed as:

$$\sigma_{\theta\theta} = \frac{1}{\sqrt{2\pi r}}\cos\frac{\theta}{2}\left[K_I\cos^2\frac{\theta}{2} - \frac{3}{2}K_{II}\sin\theta\right] + T\sin^2\theta + O\left(r^{1/2}\right) \tag{7}$$

where r and θ are the polar coordinates of the crack tip, K_I and K_{II} are the mode I and mode II stress intensity factors, respectively, and T is a constant and non-singular stress term. According to Ayatollahi et al. [30], T can be expressed as:

$$T = \frac{F_c}{\pi B R(1 - \alpha)}T^* = \frac{\sigma}{(1 - \alpha)}T^* \tag{8}$$

where F_c is the critical load, B is the thickness of the specimen, R is the radius of the specimen, α is the relative crack length, and T^* is the dimensionless form of T-stress. The high-order term $O\left(r^{(1/2)}\right)$ can be ignored near the crack tip. According to the GMTS criterion, the extreme value of Eq. (7) can be calculated from $\frac{\partial\sigma_{\theta\theta}}{\partial\theta}|_{\theta=\theta_0} = 0$:

$$[K_I\sin\theta_0 + K_{II}(3\cos\theta_0 - 1)] - \frac{16T}{3}\sqrt{2\pi r_c}\cos\theta_0\sin\frac{\theta_0}{2} = 0 \tag{9}$$

Using dimensionless F_I, F_{II}, and T^*, Eq. (9) can be simplified to:

$$[F_I\sin\theta_0 + F_{II}(3\cos\theta_0 - 1)] - \sqrt{\frac{2r_c}{a}}\frac{16T^*}{3(1 - \alpha)}\cos\theta_0\sin\frac{\theta_0}{2}$$
$$= 0 \tag{10}$$

where r_c is the critical distance at the crack tip, a performance constant of the material; and θ_0 is the crack initiation angle.

If F_I, F_{II}, and T^* are known, substituting them into Eq. (10) can calculate the crack initiation angle θ_0. Substituting the calculated θ_0 into Eq. (7) can yield:
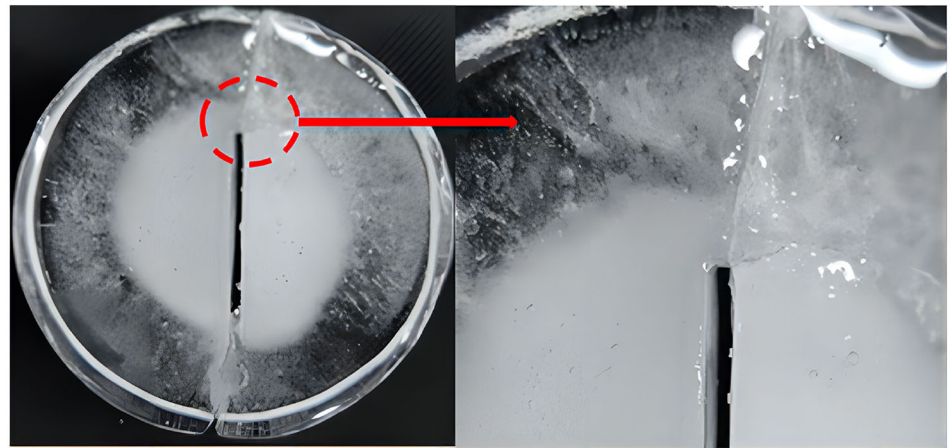
$$\sqrt{2\pi r_c}\sigma_{\theta\theta c} = \cos\frac{\theta_0}{2}\left[K_I\cos^2\frac{\theta_0}{2} - \frac{3}{2}K_{II}\sin\theta_0\right]$$
$$+ \sqrt{2\pi r_c}T\sin^2\theta_0 \tag{11}$$

From Eq. (9), it can be seen that for pure mode I, $K_{II} = 0$, and $\theta_0 = 0$. Substituting this into Eq. (9) and organizing it, we can conclude that:
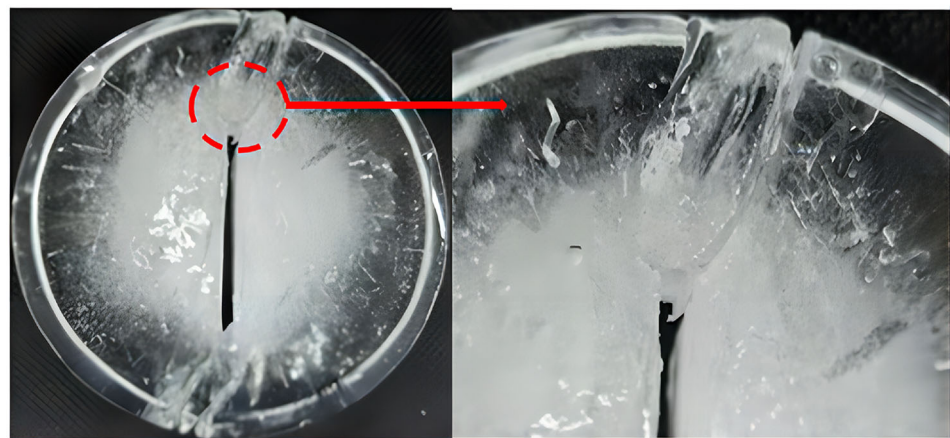
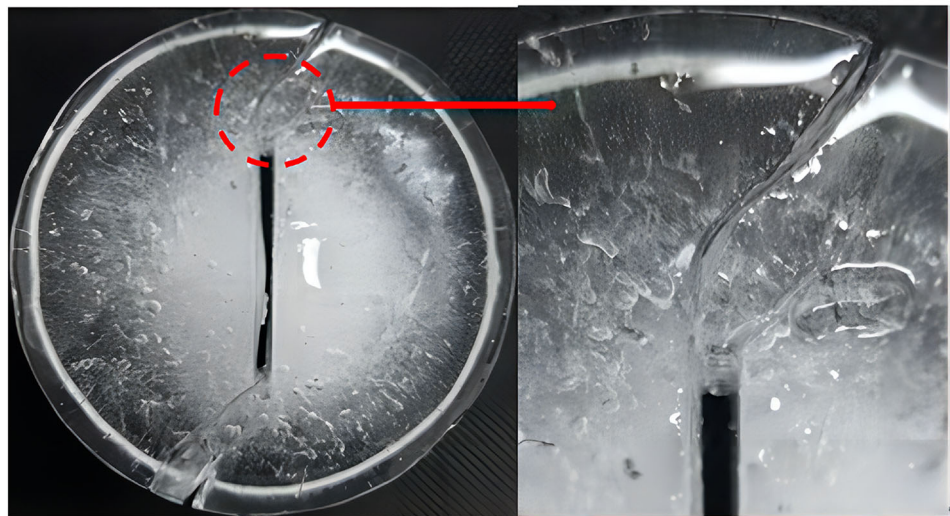$$K_{IC} = \sqrt{2\pi r_c}\sigma_{\theta\theta c} \tag{12}$$

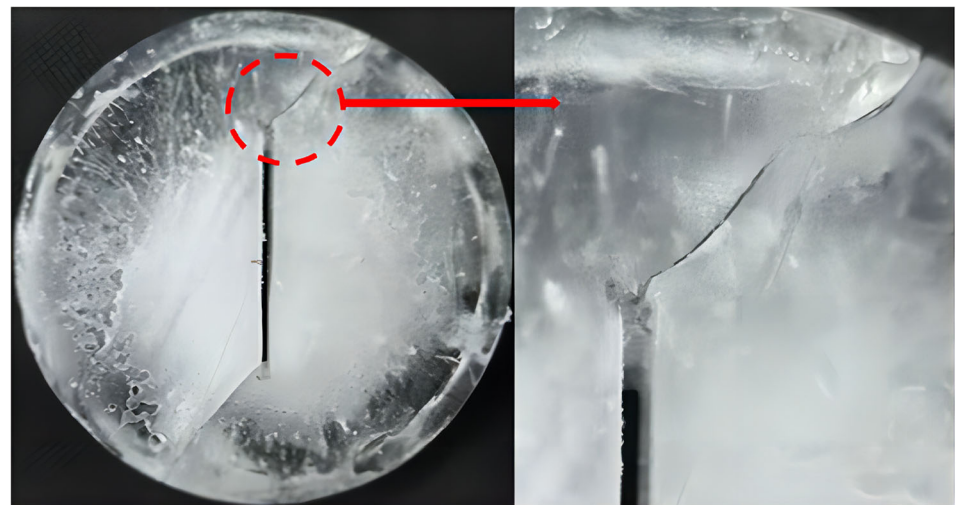**Fig. 8** Fractured forms of
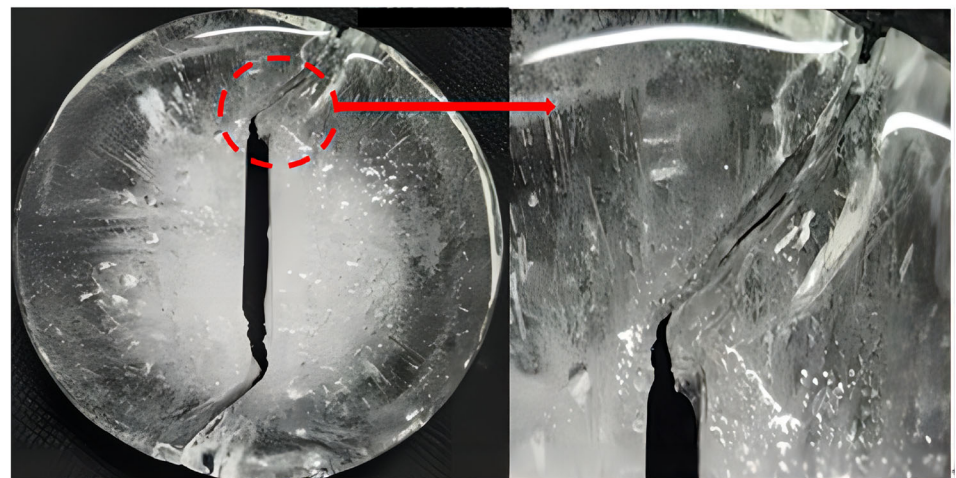specimens

(a) $\beta = 5°$

(b) $\beta = 10°$

(c) $\beta = 15°$

Fig. 8 continued

(d) $\beta = 20°$

(e) $\beta = 23°$

Then, substituting Eq. (12) into Eq. (11) and dividing it by K_I and K_{II} on both sides of the equations, we obtain:

$$\frac{K_{IC}}{K_I} = \cos\frac{\theta_0}{2}\left[\cos^2\frac{\theta_0}{2} - \frac{3}{2}\frac{K_{II}}{K_I}\sin\theta_0\right] + \sqrt{2\pi r_c}\frac{T}{K_I}\sin^2\theta_0 \tag{13}$$

$$\frac{K_{IC}}{K_{II}} = \cos\frac{\theta_0}{2}\left[\frac{K_I}{K_{II}}\cos^2\frac{\theta_0}{2} - \frac{3}{2}\sin\theta_0\right] + \sqrt{2\pi r_c}\frac{T}{K_{II}}\sin^2\theta_0 \tag{14}$$

Using dimensionless F_I, F_{II}, and T^*, Eqs. (13) and (14) can be simplified to:

$$\frac{K_{IC}}{K_I} = \cos\frac{\theta_0}{2}\left[\cos^2\frac{\theta_0}{2} - \frac{3}{2}\frac{F_{II}}{F_I}\sin\theta_0\right] + \sqrt{\frac{2r_c}{a}}\frac{T^*}{(1-\alpha)F_I}\sin^2\theta_0 \tag{15}$$

$$\frac{K_{IC}}{K_{II}} = \cos\frac{\theta_0}{2}\left[\frac{F_I}{F_{II}}\cos^2\frac{\theta_0}{2} - \frac{3}{2}\sin\theta_0\right] + \sqrt{\frac{2r_c}{a}}\frac{T^*}{(1-\alpha)F_{II}}\sin^2\theta_0 \tag{16}$$

For the experiment under mixed-mode loading discussed in this article, a CCBD specimen with a specific crack length and various loading angles is selected. The parameters obtained from the experiment are used to calculate F_I, F_{II}, and T^* and then substituted into Eq. (10) to determine the crack initiation angle θ_0. Equations (15) and (16) are used to calculate K_{IC}/K_I and K_{IC}/K_{II}. T^* is only related to the shape and loading angle of the specimen. The relationship between T^* and loading angle β can be obtained from [30–32], as shown in Fig. 9. For the CCBD specimens of freshwater ice in this article, with a relative crack length $\alpha = 0.5$, the values of T^* at different loading angles of $0°, 5°, 10°, 15°, 20°$, and $23°$ are $-2.895, -2.740, -2.317, -1.733, -$
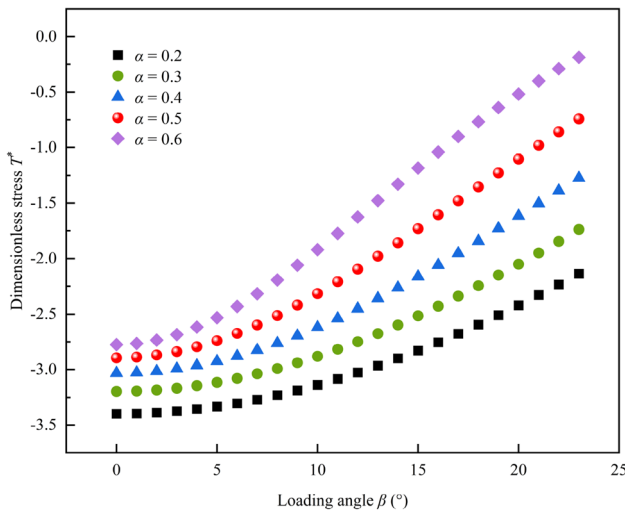
Fig. 9 The relationship between dimensionless stress T^* and loading angle β

Fig. 10 Comparison between the test results and theoretical values of mixed-mode fracture toughness

1.103, and -0.742, respectively. In Fig. 9, β is the loading angle, and T^* is the dimensionless form of T-stress. From the figure, it can be seen that for a CCBD specimen, when the relative crack length is less than 0.6, T^* is negative and increases with the loading angle β, i.e., the absolute value of T^* decreases as β increases. When the loading angle is fixed, the absolute value of T^* decreases as the relative crack length increases. The negative value of T^* reduces the magnitude of the elastic tangential stress component $\sigma_{\theta\theta}$ around the crack tip when substituted into Eq. (7). Therefore, a larger load is required to achieve the critical stress $\sigma_{\theta\theta c}$, thereby improving the load-bearing capacity of the CCBD specimen. When the loading angle is constant, a smaller relative crack length results in a greater improvement in bearing capacity. Compared to the MTS criterion, the GMTS criterion not only considers stress intensity factors but also accounts for the influence of T-stress. The presence of negative T-stress significantly reduces the crack initiation angle of the specimen, enabling a better estimation of the crack initiation angle of the specimen [23, 25].

To estimate the initiation angle as well as K_{II}/K_{IC} and K_I/K_{IC} of freshwater ice in a CCBD using the GMTS criterion, it is necessary to know the critical distance r_c at the crack tip. The calculation formula for r_c can be obtained from [3, 6, 33]:

$$r_c = \frac{1}{2\pi}\left(\frac{K_{IC}}{\sigma_t}\right)^2 \tag{17}$$

where K_{IC} represents the pure mode I fracture toughness of the material, and σ_t represents the tensile strength of the material. The tensile strength σ_t of ice obtained from the Brazilian splitting test is approximately 483 kPa. Substituting this value into Eq. (17) yields a critical distance $r_c =$

5.7 mm. Figure 10 shows a comparison between the test values of K_{II}/K_{IC} and K_I/K_{IC} of freshwater ice under mixed-mode loading conditions and the theoretical values based on the GMTS criterion. From the figure, it can be seen that the critical distance r_c significantly impacts the theoretical values of K_{II}/K_{IC} and K_I/K_{IC} based on the GMTS criterion. As r_c increases, the theoretical values of K_{II}/K_{IC} and K_I/K_{IC} also increase. When $r_c = 5.7$ mm, the experimental values and the theoretical values based on the GMTS criterion are in good agreement, indicating that the experimental results in this paper are relatively accurate. The theoretical values based on the MTS criterion have a significant deviation, mainly because the influence of T-stress is ignored. Based on the MTS criterion, the ratio of pure mode II fracture toughness to pure mode I fracture toughness $K_{IIC}/K_{IC} = 0.87$. Based on the GMTS criterion, $K_{IIC}/K_{IC} = 1.39$, while the experimental results obtained $K_{IIC}/K_{IC} = 1.6$. It can be seen that the values of K_{IIC}/K_{IC} obtained based on the GMTS criterion are in good agreement with the experimental test values, indicating that the GMTS criterion considering the influence of T-stress can better reproduce experimental results than the MTS criterion.

The theoretical values of the fracture initiation angle and fracture criterion prediction obtained from the test results are shown in Fig. 11. The actual cracking initiation angles are $13°$, $28°$, $47°$, $60°$, and $63°$, while the theoretical cracking angles predicted by the GMTS criterion are $13.47°$, $28.52°$, $45.05°$, $59.51°$, and $65.92°$, respectively. It can be seen that the error between the theoretical and test values is less than 5%. Figure 11 illustrates that the cracking angle predicted by the GMTS criterion closely aligns with the actual test results, confirming the reliability of the GMTS in contrast to the MTS criterion.
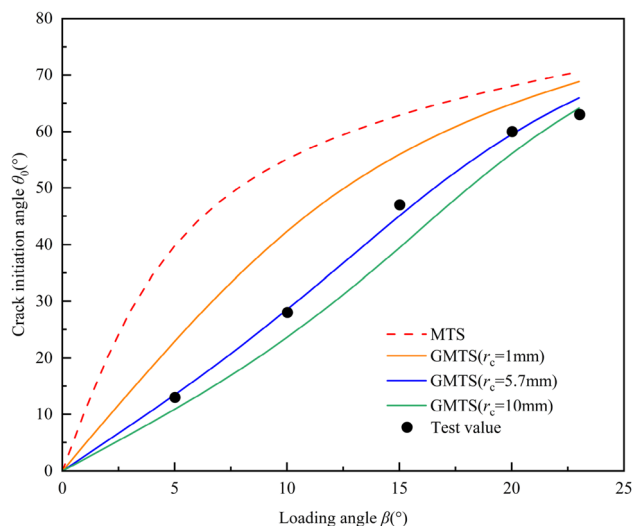
Fig. 11 Test and theoretical values of cracking initiation angles

5 Conclusion

This article presents an experimental investigation of the mode I fracture toughness and mode II fracture toughness of freshwater ice using the Brazilian test method with a CCBD specimen. We studied the fracture toughness at different loading rates and loading angles and compared the experimental results with the theoretical values of the GMTS criterion. The following conclusions were drawn:

(1) For freshwater ice, at loading rates of 1, 1.5, 2, 2.5, 3, 10, 15, and 20 mm/min, the pure mode I fracture toughness K_{IC} was found to be 137.80, 120.54, 113.18, 101.72, 91.34, 124.45, 137.28, and 180.14 kPa·m$^{0.5}$, respectively. At loading rates of 2, 2.5, 3, 4, 5, 10, 15, and 20 mm/min, the pure mode II fracture toughness K_{IIC} was 176.51, 162.92, 152.22, 137.63, 127.09, 145.75, 195.32, and 220.66 kPa·m$^{0.5}$, respectively.

(2) Under mixed-mode loading at a loading rate of 3 mm/min, with loading angles of 5°, 10°, 15°, and 20°, the mode I fracture toughness component K_I of freshwater ice was found to be 85.66, 75.61, 51.25, and 19.27 kPa·m$^{0.5}$, respectively, while the mode II fracture toughness component K_{II} was 42.04, 86.71, 123.43, and 145.63 kPa·m$^{0.5}$, respectively. K_I decreases with the loading angle β, while K_{II} increases with the loading angle β.

(3) The GMTS criterion considering the influence of T-stress yielded a ratio of $K_{IIC}/K_{IC} = 1.39$ between pure mode II fracture toughness and pure mode I fracture toughness, which is in good agreement with the experimental test value of 1.6. The theoretical values predicted by the GMTS criterion aligned well with the test values, indicating that the GMTS criterion considering the

influence of T-stress can better predict the experimental results than the MTS criterion.

Author Contributions Yaozhong Xu: Writing—original draft. Xian Yi: Investigation. Mao Zhou: Data curation. Jiuzhou Huang: Formal analysis. Wen Hua: Writing—review & editing. Wenyu Zhang: Literature research. Shiming Dong: Project administration.

Declarations

References

1. Cao Y, Wu Z, Su Y, Xu Z. Aircraft flight characteristics in icing conditions. Progress Aerospace Sci. 2015;74:62–80.
2. Smith DJ, Ayatollahi MR, Pavier MJ. The role of T-stress in brittle fracture for linear elastic materials under mixed-mode loading. Fatigue Fract Eng Mater Struct. 2001;24(2):137–50.
3. Ayatollahi MR, Aliha MRM. Fracture toughness study for a brittle rock subjected to mixed mode I/II loading. Int J Rock Mech Min Sci. 2007;44(4):617–24.
4. Ayatollahi MR, Aliha MRM. On the use of Brazilian disc specimen for calculating mixed mode I-II fracture toughness of rock materials. Eng Fract Mech. 2008;75(16):4631–41.
5. Hua W, Dong S, Xu J. Experimental study on the fracture toughness of rust stone under mixed mode loading condition. Mater Res Innov. 2015;19(sup8):S8-531-s8-536.
6. Deng Y, Li Z, Li Z, Wang J. The experiment of fracture mechanics characteristics of Yellow River Ice. Cold Reg Sci Technol. 2019;168:102896.
7. Zhang Y, Wang Q, Han D, Xue Y, Qu J, Yao H. Experimental study of the quasi-static and dynamic fracture toughness of freshwater ice using notched semi-circular bend method. Eng Fract Mech. 2021;247:107696.
8. Christmann J, Mueller R, Webber KG, Isaia D, Schader FH, Kipfstuhl S, Freitag J, Humbert A. Measurement of the fracture toughness of polycrystalline bubbly ice from an Antarctic ice core. Earth Syst Sci Data. 2015;7(1):87–92.

9. Kamio Z, Matsushita H, Strnadel B. Statistical analysis of ice fracture characteristics. Eng Fract Mech. 2003;70(15):2075–88.

10. Zhang Y, Wang Q, Han D, Li J, Wang C. Investigation on the mixed mode fracture toughness of freshwater ice using the semi-circular bend method. Cold Reg Sci Technol. 2023;205:103718.

11. Gao Z, Deng Y, Zhang P, Wang J. Evaluation of fracture behavior of Yellow River ice based on three-point bending test and PSO-BP model. Theor Appl Fract Mech. 2022;122:103644.

12. Dong S, Wang Y, Xia Y. Stress intensity factors for central cracked circular disk subjected to compression. Eng Fract Mech. 2004;71(7–8):1135–48.

13. Aliha MRM, Ashtari R, Ayatollahi MR. Mode I and mode II fracture toughness testing for a coarse grain marble. Appl Mech Mater. 2006;5:181–8.

14. Atkinson C, Smelser RE, Sanchez J. Combined mode fracture via the cracked Brazilian disk test. Int J Fract. 1982;18(4):279–91.

15. Chang SH, Lee CI, Jeon S. Measurement of rock fracture toughness under modes I and II and mixed-mode conditions by using disc-type specimens. Eng Geol. 2002;66(1–2):79–97.

16. Miarka P, Seitl S, Horňáková M, Lehner P, Konečný P, Sucharda O, Bílek V. Influence of chlorides on the fracture toughness and fracture resistance under the mixed mode I/II of high-performance concrete. Theor Appl Fract Mech. 2020;110:102812.

17. Aliha MRM, Ayatollahi MR. Rock fracture toughness study using cracked chevron notched Brazilian disc specimen under pure modes I and II loading–a statistical approach. Theor Appl Fract Mech. 2014;69:17–25.

18. Zhang Y, Wang Q, Han D, Xue Y, Lu S, Wang P. Dynamic splitting tensile behaviours of distilled-water and river-water ice using a modified SHPB setup. Int J Impact Eng. 2020;145:103686.

19. Li X, Zhang Z, Chen W, Yin T, Li X. Mode I and mode II granite fractures after distinct thermal shock treatments. J Mater Civ Eng. 2019;31(4):06019001.

20. Saksala T, Brancherie D, Harari I, Ibrahimbegovic A. Combined continuum damage-embedded discontinuity model for explicit dynamic fracture analyses of quasi-brittle materials. Int J Numer Methods Eng. 2015;101(3):230–50.

21. Zong Z. A random pore model of sea ice for predicting its mechanical properties. Cold Reg Sci Technol. 2022;195:103473–103473.

22. Dong S. Theoretical analysis of the effects of relative crack length and loading angle on the experimental results for cracked Brazilian disk testing. Eng Fract Mech. 2008;75(8):2575–81.

23. Aliha MRM, Ayatollahi MR. Analysis of fracture initiation angle in some cracked ceramics using the generalized maximum tangential stress criterion. Int J Solids Struct. 2012;49(13):1877–83.

24. Hua W, Li J, Zhu Z, Li A, Huang J, Gan Z, Dong S. A review of mixed mode I-II fracture criteria and their applications in brittle or quasi-brittle fracture analysis. Theor Appl Fract Mech. 2023;124:103741.

25. Shetty DK, Rosenfield AR, Duckworth WH. Mixed-mode fracture in biaxial stress state: application of the diametral-compression (Brazilian disk) test. Eng Fract Mech. 1987;26(6):825–40.

26. Hua W, Dong S, Pan X, Wang Q. Mixed mode fracture analysis of CCBD specimens based on the extended maximum tangential strain criterion. Fatigue Fract Eng Mater Struct. 2017;40(12):2118–27.

27. Mirsayar MM. Maximum principal strain criterion for fracture in orthotropic composites under combined tensile/shear loading. Theor Appl Fract Mech. 2022;118:103291.

28. Fakoor M, Shahsavar S. Fracture assessment of cracked composite materials: progress in models and criteria. Theor Appl Fract Mech. 2020;105:102430.

29. Sistaninia M, Ayatollahi MR, Sistaninia M. On fracture analysis of cracked graphite components under mixed mode loading. Mech Adv Mater Struct. 2014;21(10):781–91.

30. Ayatollahi MR, Aliha MRM. Wide range data for crack tip parameters in two disc-type specimens under mixed mode loading. Comput Mater Sci. 2007;38(4):660–70.

31. Fett T. Stress intensity factors and T-stress for internally cracked circular disks under various boundary conditions. Eng Fract Mech. 2001;68(9):1119–36.

32. Hua W, Li Y, Dong S, Li N, Wang Q. T -stress for a centrally cracked Brazilian disk under confining pressure. Eng Fract Mech. 2015;149:37–44.

33. Aliha MRM, Ayatollahi MR. Mixed mode I/II brittle fracture evaluation of marble using SCB specimen. Proc Eng. 2011;10:311–8.